HEFAT2014
10th International Conference on Heat Transfer, Fluid Mechanics and Thermodynamics
14 –16 July 2014
Orlando, Florida

NUMERICAL SIMULATION OF LIQUID METAL INFILTRATION AND SOLIDIFICATION INSIDE A CAPILLARY TUBE

Moussa N.[1, 2]*, Gobin D.[1], Duval H.[2] and Goyeau B.[1]

[1]EM2C Ecole Centrale Paris,
Grande Voie des Vignes,
92295 Châtenay-Malabry Cedex,
France,

[2]LGPM Ecole Centrale Paris,
Grande Voie des Vignes,
92295 Châtenay-Malabry Cedex,
France,

*Author for correspondence
E-mail: nadine.moussa@ecp.fr

ABSTRACT

A metal foam is a porous structure whose solid matrix has a large fraction of interconnected cells. The objective of our study is to define a new manufacturing process via casting that produces homogenous open cell metal foams. This comes down to studying the infiltration and solidification process of a liquid metal inside a porous mould. The metal foams are characterized by their high porosity and permeability values; thus, the size of the mould pore is small enough to be considered as a capillary tube. Therefore, the focus of this paper is on modelling and numerical simulation at the local scale of the infiltration and solidification of liquid metal inside a capillary tube. For this matter, a one-domain approach is chosen.

The defined mathematical model is implemented in a CFD tool: OpenFOAM [1]. A numerical validation is performed by comparing the numerical results with well-known solutions of test cases. Subsequently, a numerical parametrical study enabled us to find the relationships between the penetration length of the liquid metal before solidification and the infiltration time as function of the metal initial superheat and of the mould preheated temperature, two operational parameters of importance in the process.

INTRODUCTION

The competitiveness in the metal industry leads to severe products specifications in order to reduce the cost of the manufacturing process. Thus, metal foams present a promising material since it keeps the high mechanical properties of the metal while reducing the weight up to 90%. Metal foam has a variety of applications depending on whether the cells are connected or not; e.g. open-cells foams are used in heat exchangers to increase heat transfer, while closed-cells foams are employed as impact-absorbing material such in vehicle's crash box. Several patented manufacturing processes have been introduced during the last two decades [2-4]. However, the metallic melts are foamed either by injecting gas into liquid or by the use of blowing agents. As a result, the structure of the foam, its homogeneity and its effective properties cannot be rigorously controlled.

The CTIF [5] presented a manufacturing process of metal foam via casting CastFoam® [6] that produces well defined homogenous foams. In particular, this process is able to produce perfectly regular foams made of Kelvin cells. However, this process needs to be optimized before being employed in the metal industry. Thus, the infiltration and solidification of liquid metal inside the porous mould must be

studied. Metal foams obtained using this process have high permeability and porosity values; hence the size of the mould pore is small and can be modelled as a capillary tube. Subsequently, our objective is to study the infiltration and solidification of liquid metal in a capillary tube.

Metal foams may be made of steel, copper, nickel and aluminium. However, the latter is the most widely used in industrial processes because of its low density and its good mechanical properties. Moreover, its fusion temperature is much lower than the other materials, which makes the manufacturing process less expensive and easier to handle. Therefore, liquid aluminium is chosen in our numerical study as well as in the validation experiments.

NOMENCLATURE

ρ	[kg/m^3]	Density
μ	[Pa.s]	Dynamic viscosity
k	[W/mK]	Thermal conductivity
cp	[J/kgK]	Heat capacity
σ	[N/m]	Surface tension
K	[m^{-1}]	Curvature
$\mathbf{v}$	[m/s]	Velocity vector
p	[Pa]	Pressure
T	[K]	Temperature
θ	[K]	Temperature integration variable
T_s	[K]	Solidus temperature
T_l	[K]	Liquidus temperature
ε	[K]	10^{-6}
H	[KJ/ m^3]	Enthalpy
L	[J/ m^{3}K]	Latent heat
L_m	[m]	Mechanical entrance length
L_{th}	[m]	Thermal entrance length
D	[m]	Tube diameter
r	[m]	Radius
Re	[-]	Reynolds number
Pr	[-]	Prandtl number
Nu	[-]	Nusselt number

Special characters

α	[-]	Metal volume fraction
g_l	[-]	Liquid metal fraction
ϕ	[-]	Mould indicator
A	[kg/m^{3}s]	Solid metal penalty coefficient
B	[kg/m^{3}s]	Mould penalty coefficient
C	[kg/m^{3}s]	Large constant ($\sim 10^{20}$)
D	[kg/m^{3}s]	Large constant ($\sim 10^{30}$)

Subscripts

l	Liquid metal
s	Solid metal
$metal$	Metal
g	Gas
m	Mould
$melt$	Melt
r	Relative
ref	Reference
in	Inlet
out	Outlet

MATHEMATICAL MODEL

The liquid metal infiltration and solidification inside a capillary tube is handled by solving the governing equations presented in this section, using a one-domain approach. The fluid flow is governed by the modified Navier-Stokes equation for an incompressible fluid. Therefore, the continuity and the momentum equations are given by:

$$\frac{\partial \rho}{\partial t} + \nabla . (\rho \mathbf{v}) = 0 \tag{1}$$

$$\frac{\partial (\rho \mathbf{v})}{\partial t} + \nabla . (\rho \mathbf{v}\,\mathbf{v}) = -\nabla p + \nabla (\mu \nabla \mathbf{v}) + \sigma K \nabla \alpha - A\mathbf{v} - B\mathbf{v} \tag{2}$$

where $K = -\nabla \left(\frac{\nabla \alpha}{|\nabla \alpha|} \right)$ is the curvature of the metal-gas interface.

In the two-phase flow model, the momentum equation contains an additional source term which is the pressure jump at the liquid-gas interface arising from the surface tension between the two fluids. Using the volume-of-fluid (VOF) method [7] this term (the third term in the RHS of eq. (2)) is evaluated by resolving the transport equation of the metal volumetric fraction α:

$$\frac{\partial \alpha}{\partial t} + \nabla . (\mathbf{v}\,\alpha) + \nabla . \left[\mathbf{v_r}\, \alpha\, (1-\alpha) \right] = 0 \tag{3}$$

where $\mathbf{v_r} = \mathbf{v_l} - \mathbf{v_g}$ is the relative velocity of the two fluids.

The surface curvature is a function of the volumetric fraction and is required for the determination of the surface tension force. Therefore, the calculation of the volumetric fraction distribution must be accurate especially in the case of high physical properties ratios (density, thermal conductivity...), where small errors in evaluating the volumetric fraction lead to significant errors in calculating the effective physical properties. Thus, equation (3) contains an additional convective term known as the compression term active only within the interface region where $\alpha(1-\alpha) \neq 0$; its role is to get a sharper liquid-gas interface [7]. As we can see, the momentum equation contains also two supplementary terms, which will be discussed later on after presenting the solidification model.

For the modelling of phase change of the metal we use a modified enthalpy-porosity method [8]. The advantage of this method is that it respects the one domain approach. The energy conservation equation is written as follow:

$$\frac{\partial H}{\partial t} + \nabla . (\mathbf{v}\, H) = \nabla . (k \nabla T) \tag{4}$$

The latter contains two depending variables, but the enthalpy may be written as function of temperature and of different volumetric fractions fractions:

1. ϕ the mould indicator

$$\phi = \begin{cases} 0 & \text{mould} \\ 1 & \text{air or metal} \end{cases}$$

2. α the metal/air fraction

$$\phi = 1, \quad \alpha = \begin{cases} 0 & \text{air} \\ 1 & \text{metal} \end{cases}$$

3. g_l the liquid fraction

$$\phi = 1, \quad \alpha = 1, \; g_1 = \begin{cases} 0 & \text{solid} \\ 1 & \text{liquid} \end{cases}$$

$$H = \phi \left[\alpha \left(g_l \int_{T_{ref}}^{T} \rho_l \, c_{Pl} \, d\theta + \rho_l \, g_l \, L \; + (1 - g_l) \int_{T_{ref}}^{T} \rho_s \, c_{Ps} \, d\theta \right) + (1 - \alpha) \int_{T_{ref}}^{T} \rho_g c_{Pg} d\theta \right] + (1 - \phi) \left[\int_{T_{ref}}^{T} \rho_m \, c_{Pm} \, d\theta \right] \tag{5}$$

Deriving the enthalpy expression with respect to time and space and replacing it in equation (4) gives the following energy equation:

$$\rho \, c_P \frac{\partial T}{\partial t} + \rho \, c_P \nabla . (\mathbf{v} \, T) = \nabla . (k \, \nabla T) - \phi \, \alpha \, \rho_l \, L \frac{\partial g_l}{\partial t} - \phi \, \alpha \, \rho_l \, L \nabla . (\mathbf{v} \, g_l) \tag{6}$$

In the case of an isothermal phase change, the convective term of the liquid fraction is null, because there is a sharp interface between the liquid and solid phases and the fluid velocity at the interface is zero [9]. The solidification of a pure metal is assumed to be isothermal, therefore the final form of the energy equation is:

$$\rho \, c_P \frac{\partial T}{\partial t} + \rho \, c_P \nabla . (\mathbf{v} \, T) = \nabla . (k \, \nabla T) - \phi \, \alpha \, \rho_l \, L \frac{\partial g_l}{\partial t} \tag{7}$$

The liquid metal fraction is a linear function of temperature [10]:

$$g_l = \begin{cases} 0 & T < T_s \\ \dfrac{T - T_s}{\varepsilon} & T_s \le T \le T_l \\ 1 & T > T_l \end{cases} \tag{8}$$

where $\varepsilon = T_l - T_s$, the temperature difference between the liquidus and solidus, is taken to have a small value (10^{-6} K), so that the liquid fraction will approach a Heaviside step function.

In a one domain approach, the four domains (mould, air, liquid and solid metal) are considered as one effective fluid throughout the domain having physical properties weighted as function of the phase fractions:

$$\rho = \alpha \, \rho_{metal} + (1 - \alpha) \, \rho_g \tag{9}$$

$$\mu = \alpha \, \mu_l + (1 - \alpha) \, \mu_g \tag{10}$$

$$\rho c_p = \phi \left[\alpha \, \rho_{metal} \left(g_l \, c_{Pl} + (1 - g_l) \, c_{Ps} \right) + (1 - \alpha) \rho_g c_{Pg} \right] + (1 - \phi) \left[\rho_m c_{Pm} \right] \tag{11}$$

Note that here we assume that the density difference between the liquid and solid phases is negligible.

These effective properties are obtained by assuming a linear variation between the physical properties of each phase at the different interfaces. However, this simple relation cannot be used when calculating the effective conductivity because of the high ratio between the metal and air conductivity values. Therefore, using Patankar [11] formulation, the effective conductivity is given by:

$$k = \phi \left[\frac{\alpha}{(g_l \, k_l + \, (1 - g_l) \, k_s)} + \frac{(1 - \alpha)}{k_g} \right]^{-1} + (1 - \phi) \left[k_m \right] \tag{12}$$

The local volume fractions are used to define the penalty terms in the momentum equation (2). The first source term imposes a zero velocity field in the solidified metal, using a penalty coefficient A that acts only in the metal region and is function of the liquid metal fraction:

$$A = \alpha \, \phi \, C \, (1 - g_l) \tag{13}$$

When the calculated temperature T is higher than the melting temperature, the liquid metal fraction is equal to 1 and the penalty coefficient vanishes, thus the momentum equation recovers its normal form. Alternatively, when the calculated temperature is lower than the melting temperature, solidification occurs and the liquid metal fraction is equal to zero. Thus, the penalty coefficient has a large value and results in a zero velocity field.

The second additional source term in the momentum equation ensures a zero velocity field in the mould region. Thus, the penalty coefficient is function of the mould indicator:

$$B = (1 - \phi) \, D \tag{14}$$

In the air/metal domains ϕ = 1 and the penalty coefficient turns to zero. However, in the mould region ϕ = 0 and the penalty coefficient has a large value ensuring a zero velocity solution.

NUMERICAL PROCEDURE

The mathematical model presented earlier is implemented in a CFD open source software OpenFOAM [1]. The source code is written in C++ for Linux operating systems and contains essential modules to solve flow and heat transfer problems. It uses the finite volume method where the space is divided into discrete control volumes, and time is split into a number of time-steps. The solution procedure of the transient equations can be summarized as follows: first a computationnal mesh is generated, and the variable fields are initialized. Then, the time loop starts, and the time step is calculated in order to satisfy the Courant-Friedrichs-Lewy (CFL) condition. After that, the transport equation of the metal volume fraction (3) is solved, which enables us to calculate the surface tension force. Subsequently, the metal-gas interface is constructed and the physical properties are updated as functions of the fractions eqs. (9-12). Next, the pressure-velocity coupling is solved using the PIMPLE (PISO-SIMPLE) scheme of OpenFOAM for the continuity and the momentum equations (1, 2). Afterwards, the convergence of the solution is monitored by calculating the error on the velocity divergence. At this stage, the pressure and velocity fields as well as the metal fraction distribution are known for the current time step. Using the velocity field solution, the energy equation (6) can now be solved to obtain the temperature field and the liquid metal fraction g_l, which is used to update the penalty source term of the momentum equation. Now all the variable fields are known, if the final time is not reached yet, the time loop continues with the calculation of the next time step.

Validation

The numerical validation of the code is done by comparing the 2D numerical solutions with analytical solutions for simple test cases available in the literature. In this section, the mould is not taken into consideration. The capillary tube is modelled as a cylindrical tube of 1.2 mm radius, and 120 mm length (unless mentioned differently) to be in accordance with the pore size of a typical metal foam mould and of the tube diameter used in the fluidity tests. The mesh (see Figure 1) consists of a structured 2D radial quadrangle extruded to 3D and generated using Salome software [12].

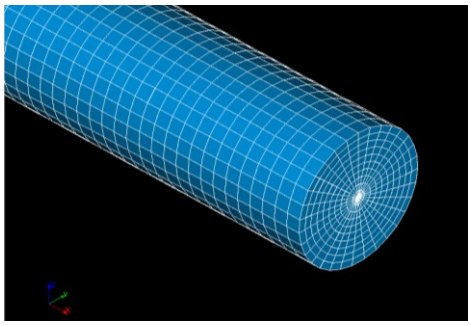

Figure 1 Global view of the geometry and mesh of the tube

1. Convection problem

The first step of our code validation is done by simulating an isothermal one-phase flow and comparing it to the Poiseuille solution. The tube is initially filled with liquid aluminium at a temperature higher than its fusion temperature and a zero thermal flux is set at the tube wall. A Dirichlet boundary condition of constant uniform velocity profile is imposed at the inlet. The dimensionless Reynolds number is taken equal to 600, which corresponds to an average velocity of 0.1 m/s.

The radial velocity profile in a cross section beyond the entrance length (x=100 mm) is in good agreement with the Poiseuille solution, and the relative error on the maximum axial velocity is less than 1%.

For an isothermal two-phase flow the metal-air interface is tracked, and a special attention is given to the interface velocity. In fact, after a certain time the interface shape remains the same, and displaces at the fluid mean velocity; as stated by Dussan [13] "the speed of the contact line $Q/\pi a^2$". In order to understand the motion of the two fluids and the interface dynamics we refer to [13] where it is demonstrated that the displacing fluid undergoes a rolling motion and that the displaced fluid has a similar but more complex behaviour. To visualize this, the relative velocity vectors in the interface frame of reference are shown below:

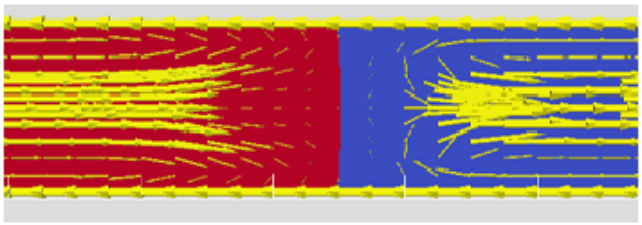

Figure 2 Relative velocity vectors in the region of the liquid-gas interface

Figure 2 shows that the displacing fluid flows forward at the tube centre, and then rolls out at the interface vicinity to flow on backward near the wall. At the other hand, the displaced fluid flows backward near the wall, and rolls in at the interface to flow forward at the tube centre. This rolling motion explains why in the fluid regions (liquid and gas) we have a parabolic radial velocity profile where the fluid flows faster at the tube axe and slower near the tube wall and a constant radial velocity profile at the metal-air interface.

After validating the hydrodynamic behaviour of one-phase flow, now the thermal aspect should be verified. Therefore, an internal forced convection is simulated. There are two possibilities of thermal conditions at the tube wall: fixed temperature or constant thermal flux, accordingly to which the thermal entrance length and the correlated dimensionless number of Nusselt are given. Using the aluminium properties, the thermal entrance length for both cases is negligible in comparison with the mechanical one. The validation of the thermal behaviour is done by fixing a constant flux at the wall. The radial temperature profile obtained at a cross section beyond the thermal and mechanical entrance lengths (x = 100 mm) gives a Nusselt number of 4.3 to be compared to the usual

correlation Nu = 4.363 [14], giving a relative error less than 1.5%.

2. Phase change

An analytical solution for inward solidification in a cylinder for a liquid initially at the fusion temperature may be found in literature [15]. The numerical solution is compared to the one-dimensional pure conduction analytical solution: a negative uniform heat flux is imposed at the outer boundary of a cylindrical tube filled with a liquid at its melting temperature. The radial position of the solid-liquid interface as function of time obtained numerically and analytically is shown in the figure below.

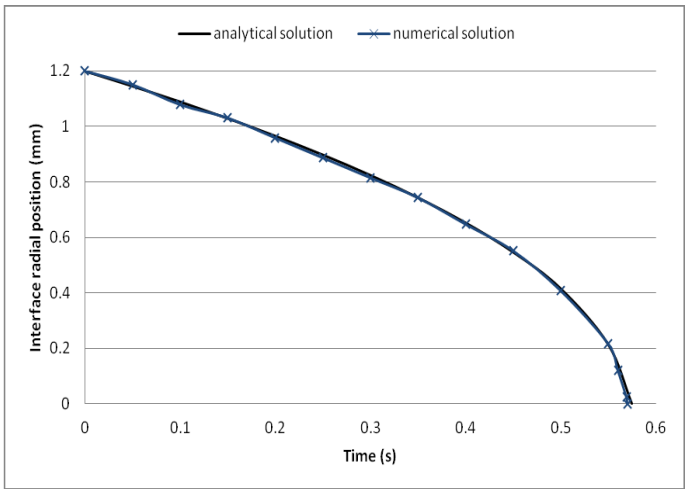

Figure 3 Solid-liquid interface position as function of time

As can be seen,

Figure 3 shows a good agreement between the numerical and analytical solutions. However due to the use of the enthalpy method for solving a phase change problem for a pure material, the mesh size and the time step must be carefully chosen to avoid stepwise evolution of the front position.

The temperature profiles at various times are also in very good agreement and this test is admitted to validate the ability of the code to describe the solidification process with good accuracy.

RESULTS AND DISCUSSION

Solidification dynamics

The numerical code is now used to study the solidification dynamics of a fluid flowing in a capillary tube in various configurations. In a first step, we study the solidification coupled to diffusion-convection heat transfer in a tube without external mould. A 1.2 mm radius and 50 mm long tube is initially filled with liquid aluminium at a temperature of 975 K, and the flow is driven by a pressure difference of 300 Pa between the tube inlet and outlet. Solidification is provoked by extracting a constant heat flux of -1000 kW/m^2 at the external wall. The imposed heat flux is uniform and the effect of gravity is neglected, thus an axi-symmetrical solidification is expected.

The evolution of the solidification process is shown in Figure 4 below.

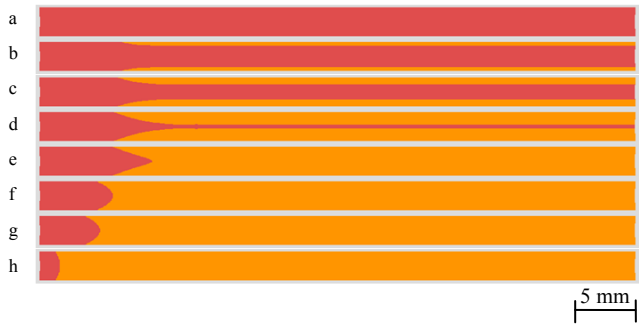

Figure 4 Solidification process of liquid aluminium (liquid phase in red, solid phase in orange);
a. (t = 0s) - initially the tube is completely filled with liquid aluminium,
b. (t = 0.07 s)- aluminium solidification starts at the tube wall at a distance from the entry,
c. (t = 0.073 s), d. (t = 0.076 s) - the solidified aluminium progresses in the radial direction,
e. (t = 0.077 s) – the solidified aluminium obturates the tube at a distance from the inlet and stops the fluid flow,
f. (t = 0.09 s), g. (t = 0.1 s)- solidification proceeds by diffusion towards the entry,
h. (t = 0.15 s) - complete solidification is achieved.

The solidification process of the liquid aluminium could not be validated against a reference solution, but the order of magnitude of the infiltration time compares well with experiments performed at CTIF [5].

Our second objective is to describe the solidification process during the infiltration of a cylindrical mould by liquid aluminium. Thus, we now consider that the tube is initially filled with air and is inserted in a sand mould through which it will be cooled. The cylindrical mould has an annular cross section with an inner radius of 1.2 mm and an outer radius of 5 mm. The mould external wall is adiabatic (zero thermal flux) and the initial mould and air temperature is 294 K (unless mention differently). The liquid aluminium flow is driven by a constant pressure difference of 1400 Pa, sufficient to overcome the Laplace pressure at the metal-air interface. We consider a superheated metal initially at T = 1045 K (ΔT = 112 K above the solidification temperature), which corresponds to an intermediate value of the Stefan number (0.33). This means that the involved sensible heat is lower, but comparable, to the latent heat of the metal. The result of this numerical simulation is shown in Figure 5.

In a first step, the liquid metal infiltrates the tube and rejects the air outside. The aluminium, remains liquid as long as it loses its initial superheat, solidification starts at the metal-mould contact in the vicinity of the metal-air interface a zone which has exchanged heat with the outside on a longer time. As the metal flows in the mould, solidification proceeds in both axial and radial directions, until the flow is blocked up (t = 0.43 s) when the solid crust closes the tube at 4 mm upstream of the metal-air interface. This behaviour is expected, since the metal close to the air interface is constantly in contact with the cooler mould, so that the temperature decreases in this region is more important. After immobilization of the liquid phase, we can

observe diffusive phase change with axial solid growth until the whole metal domain is completely solidified (t = 3s). In the present case, the length of mould filled with solid metal is 162 mm.

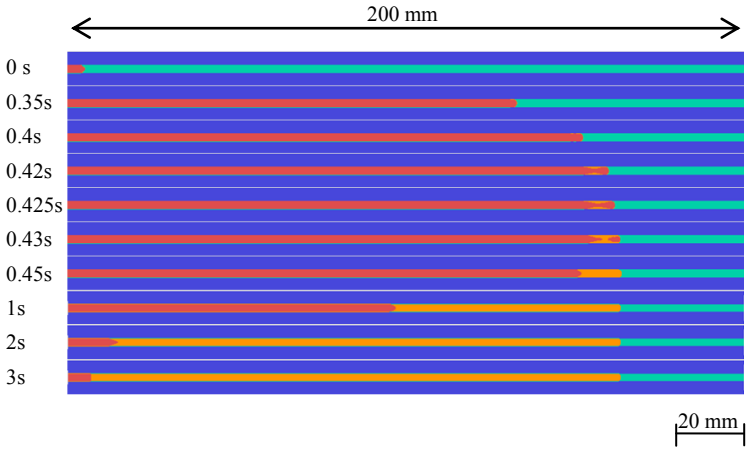

Figure 5 Liquid aluminium infiltrating a cylindrical mould; liquid phase (red), solid phase (orange), mould (blue), air (cyan)

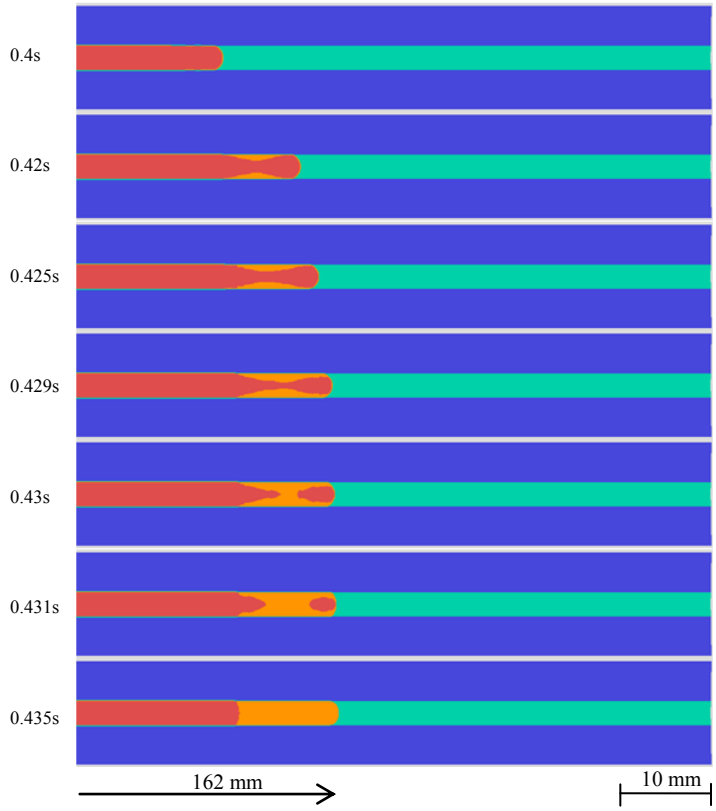

Figure 6 Liquid aluminium solidification during infiltration of a capillary tube; liquid phase (red), solid phase (orange), mould (blue), air (cyan)

In order to observe in more detail the solidification process, a zoom of the solidification zone is shown in Figure 6.

One clearly sees that solidification is initiated at the liquid-mould contact a few mm from the air-liquid interface, which slows down the fluid flow and increases the heat exchange with the mould. The solidified zone progressively expands along the tube and in the radial direction until complete blockage. The liquid flow is then stopped and solidification proceeds in the upstream direction by pure heat diffusion.

Influence of the operational conditions

The latter configuration is intended to schematically simulate the infiltration of the pores of a porous mould by a solidifying liquid metal. The thickness of the mould has been chosen so that it may absorb the latent heat contained in the initial liquid without an excessive mould temperature rise. Since, the system is supposed to have negligible heat losses towards the ambient.

Under these assumptions, the code may be used to study the influence of some of the process parameters, namely the injected liquid temperature and the mould preheating, on important indicators of the process: infiltrated length and the infiltration time. For the same thermal and hydrodynamic conditions as above, these parameters are changed and four values of the metal superheat and mould preheat temperature are used.

The mould and air are considered at ambient temperature; only the metal initial superheat is changed. The values of the injection temperature are those used in the fluidity tests (985 K, 1045 K, 1105 K and 1155 K), corresponding to initial superheat of 52 K, 112 K, 172 K, 222 K respectively. The effect of this parameter on the infiltrated length and infiltration time are shown in the plots in Figs. 7 and 8.

As expected, the infiltrated length (and thus the infiltration time) increases with the initial temperature of the liquid. The plots show a quasi linear variation in the range of values under consideration. In the casting process, this information may be relevant to the mould conception.

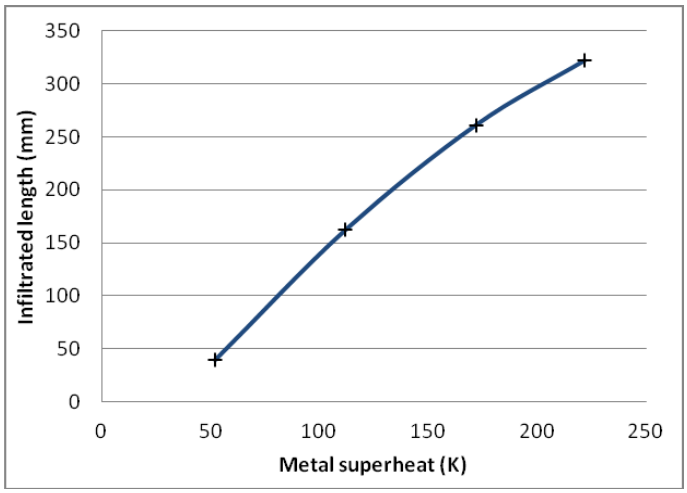

Figure 7 Effect of initial superheat on the infiltrated length

Then, in the same way the dynamics of the problem is also depending on the initial thermal state of the mould, since it determines its ability to cool and solidify the liquid metal. We thus consider different values of the mould temperature (294 K, 450 K, 600 K and 800 K) for an initial superheat of 52 K (T = 985 K). The results are shown in Figure 9.

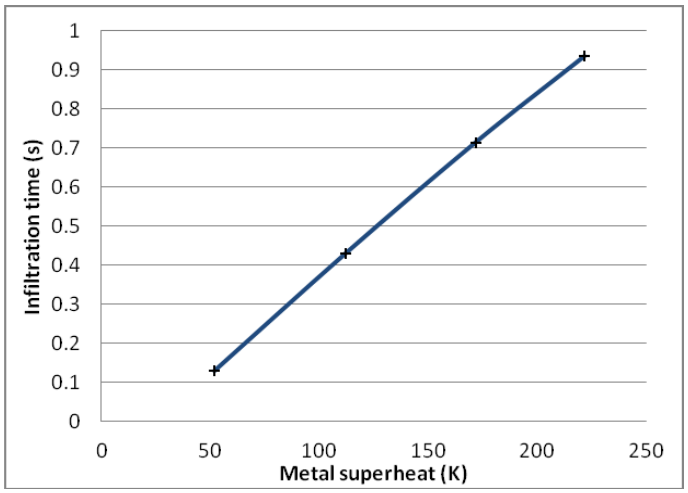

Figure 8 Effect of initial superheat on the infiltration time

Again, the infiltration length is very sensitive to the initial mould temperature. The plots show that when the mould is preheated to a higher temperature, the liquid metal infiltrates greatly the tube, because at high temperatures the mould cannot easily evacuate the heat from the liquid. A more complete analysis should be done by changing the boundary condition on the external wall of the mould in order to account for possible heat losses.

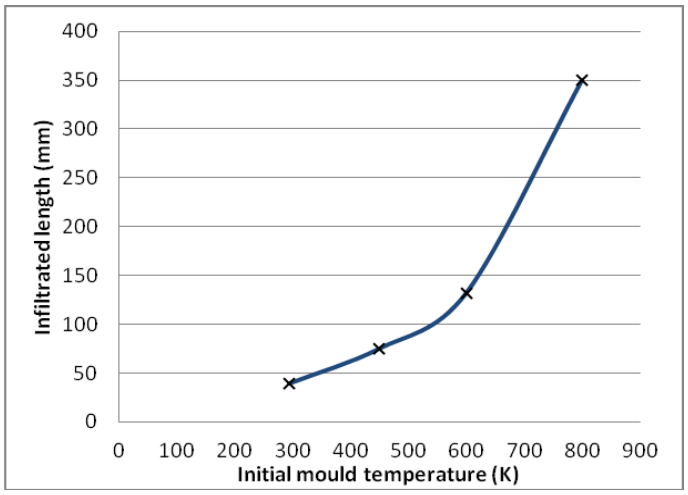

Figure 9 Effect of initial mould temperature on the infiltrated length (injection temperature: 985 K)

In our upcoming work, the parametric study will be extended to include the effect of the pressure difference between the tube inlet and outlet. And the model still has to be validated against experimental results. The experimental tests currently under preparation will use two different metals: aluminium and copper.

CONCLUSION

The infiltration of a cylindrical mould by a solidifying liquid metal has been simulated numerically. The physical behaviour of the process is successfully represented. The present extension of this study is to identify the effect of the pressure difference on the infiltration length and solidification time, a key parameter to determine optimal operating conditions of infiltrating a porous mould in the metallic foams manufacturing process.

This work is the first step of the modelling approach, where we intend to propose a macroscopic model of the coupled infiltration-solidification process of the porous mould by deriving the volume-averaged equations from the local scale model using a volume averaging method [16]. Then, the effective properties will be determined by resolution of the closure problems and the macroscopic equations will be implemented in a CFD software; subsequently the numerical results will be compared to the metal foam casting tests.

ACKNOWLEDGEMENT

The authors wish to acknowledge the financial support of the MATETPRO Program of the French National Research Agency under FOAM project (ANR - 2010- RMNP- 018).

REFERENCES

[1] www.openfoam.com
[2] T. Miyoshi, M. Itoh, S. Akiyama, and A. Kitahara, ALPORAS Aluminum Foam: Production Process, Properties, and Applications, *Adv. Eng. Mater.*, vol. 2, no. 4, 2000, pp. 179–183.
[3] www.alusion.com/home.html
[4] www.ergaerospace.com/index.html
[5] www.ctif.com
[6] www.alveotec.fr/innovation.html
[7] H. Rusche, Computational Fluid Dynamics of Dispersed Two-Phase Flows at High Phase Fractions, 2002.
[8] A. D. Brent, V. R. Voller, and K. J. Reid, The Enthalpy-Porosity Technique For Modeling Convection-Diffucion Phase Change : Application To The Melting Of A Pure Metal, *Num. Heat Transf.*, vol. 13, 1988, pp. 297–318.
[9] V. R. Voller and C. Prakash, A fixed grid numerical modelling methodology for convection-diffusion mushy region phase-change problems, vol. 30, 1987.
[10] F. Rösler and D. Brüggemann, Shell-and-tube type latent heat thermal energy storage: numerical analysis and comparison with experiments, *Heat Mass Transf.*, vol. 47, Jul. 2011, pp. 1027–1033.
[11] V. Patankar, Numerical Heat Transfer and Fluid Flow, 1980.
[12] http://www.salome-platform.org
[13] E. B. Dussan V., On the spreading of liquids on solid surfaces: static and dynamic contact lines, *Ann. Rev. Fluid Mech.*, vol. 11, 1979, pp. 371–400.
[14] J. Padet, Convection thermique et massique Nombre de Nusselt: partie 1, *Tech. Ing.*, BE 8206, 2005.
[15] V. Alexiades and Alan D. Solomon, Mathematical Modeling Of Melting And Freezing Processes. *CRC Press*, 1992, p. 144-147.
[16] S. Whitaker, *The Method of Volume Averaging*. Kluwer Academic Publishers, 1999.